International Journal of Progressive Sciences and Technologies (IJPSAT)
ISSN: 2509-0119.

http://ijpsat.ijsht-journals.org
Vol. 22 No. 2 September 2020, pp. 290-303

Quantum−Mechanical Investigation of Chemical Energetics and Electronic Stabilities of Microhydrated Protons [$H^+(H_2O)_n$]

Anant Babu Marahatta[1, 2]

[1]Department of Chemistry, Amrit Science Campus, Tribhuvan University, Kathmandu, Nepal
[2]Chemistry Subject Committee, Kathford International College of Engineering and Management (Affiliated to Tribhuvan University), Kathmandu, Nepal

Abstract – Though proton hydration is a spontaneous phenomenon that occurs as a result of reorientation of the polar H_2O molecules in the immediate vicinity of the proton, its ultimate role to give rise to an unusually high diffusion rate of the protons in batteries, fuel cells, and Nafion series proton exchange membranes has captivated the interest of researchers for a long time. Interestingly, such anomalously high proton conductivity is already found to be caused due to the formation of several hydrated states of the protons out of which most possible stable states are hydronium (H_3O^+), zundel ($H_5O_2^+$), and eigen ($H_9O_4^+$) cations. This study is mainly aimed to probe deep into the molecular−level of these three hydrated protons by applying DFT−based quantum mechanical model, and to unveil their electronic stabilities, ground state electronic structures/ energies, binding energies, and relative thermodynamic stabilities theoretically. The DFT derived ground state electronic structures of them are observed as flattened like a wind−blown umbrella, linear and flat, and triangular planar shape respectively. All these three 3D geometries are examined quantitatively through electron density mapping (mapped with the total density) techniques, and found no structural deviations. Besides this, the relative thermodynamic stability of them is closely monitored and found the order as $H_9O_4^+ > H_5O_2^+ > H_3O^+$. The significance and originality of this study lies in enlightening most of the structural and energetic properties of the three most stable hydrated states of the protons, and in producing their structural data sets that are very essential while modeling fuel cell and redox flow battery simulators.

Keywords – Hydrated protons, Electronic stability, Binding energy, and Thermodynamic stability.

I. INTRODUCTION

One of the most significant characteristic properties of the pure water containing H_2O molecules is their ability to dissociate spontaneously into an equivalent amount of H^+ and OH^- ions (H_2O (l) ⇌ H^+ (aq) + OH^- (aq)). The main reason behind this is that 1×10^{-7} moles of H_2O present in one liter of pure water donates proton (Bronsted acids) to another 1×10^{-7} moles of H_2O molecules (Bronsted bases) giving exactly the same amount of H_3O^+ and OH^- ions (H_2O (l) + H_2O (l) ⇌ H_3O^+ (aq) + OH^- (aq)) [1]. In the aqueous solution, a spontaneously generated proton (H^+) bearing exceptionally high charge density (2×10^{10} that of Na^+) attracts lone pair electrons of the oxygen atom of nearby H_2O molecule (conjugate base) ($H^+ + H_2O \rightarrow [H_2O{\rightarrow}H^+]$ or $[H_3O^+]$), and generates one of the stable hydrated states of the proton called hydronium ion H_3O^+ (conjugate acid of H_2O) [1], [2] as displayed in **chart 1(a)**. It means, the interactions between them is so intense that a bare hydrogen ion never got a chance of existing alone in the massive excess of H_2O molecules in the aqueous type media. The very interesting and captivating fact of their coordination or conjugation is that the H^+ ion never sticks to single H_2O molecule instead it diffuses through the channel of hydrogen bonded H_2O networks by changing its H_2O (conjugating) partners many times per second (Grotthuss mechanism) [3]. Contrastingly, the proton

Corresponding Author: Anant Babu Marahatta

Chart 1

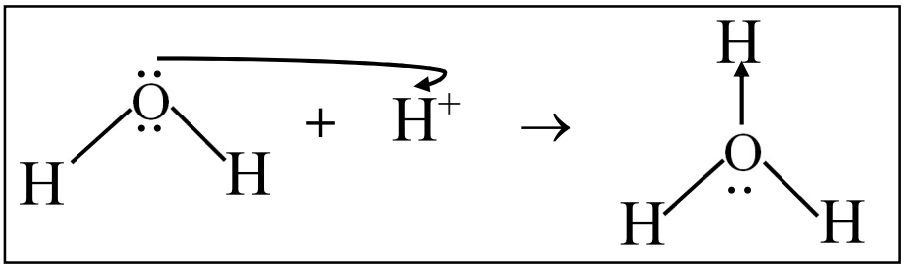

(a) Hydronium ion (H_3O^+)

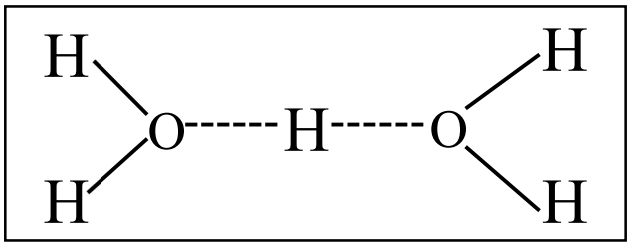

(b) Zundel ion ($H_5O_2^+$)

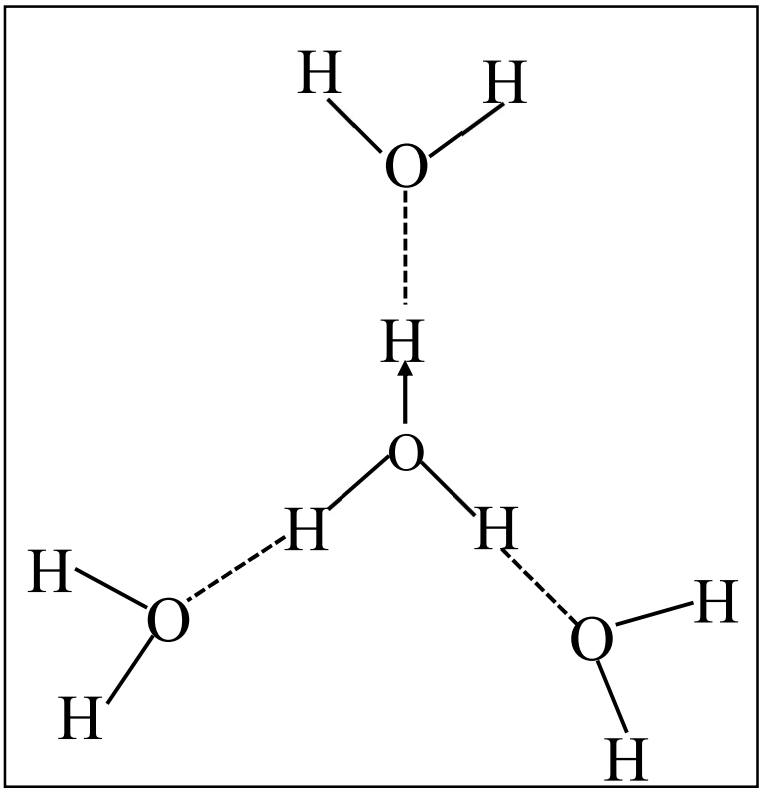

(c) Eigen ion ($H_9O_4^+$)

carrying H_2O (i.e. in the form of H_3O^+) also moves itself as a proton−attached molecular vehicle from one place to another, and transports proton through vehicular mechanism [3], [4]. In fact, the former indirect "without real movement

of the H_3O^+ unit ", and the latter direct "real movement of the H_3O^+ unit" diffusion mechanisms of the protons are responsible for the extraordinarily high electrical conductivity of the acidic aqueous solutions. Thus, a self−dissociation or an auto−ionization process of H_2O molecules even in an ultrapure water system is their very typical and strange feature which plays crucial role not only to enhance ionic conductivity and ionization plus dissolution processes of strong and weak electrolytes (acids, bases, and salts) but also to initiate several acid−base type chemical reactions, to ease proton hopping in several types of proton exchange semipermeable membranes while incorporating into the membrane electrode assembly, and to understand ionic transport phenomena in all the pH−related chemical, biological, industrial, environmental, and catalytic aqueous systems.

According to infrared spectroscopy, an H_3O^+ ion present in water affects the hydrogen− bonding network of at least one hundred surrounding H_2O molecules [4]. This is because of its strong tendency to share one to three H atoms for forming one to three hydrogen bonds (hereafter, H−bond) with nearby H_2O molecules. The most worthy point is that the strength of these donated H−bonds are reported twice as strong as those present in between H_2O molecules of the bulk water, implying that other stable hydrated states of proton such as zundel $H_5O_2^+$ and eigen $H_9O_4^+$ exist in the aqueous type solutions [5]. Structurally, the zundel cation is formed as a result of binding one H_3O^+ ion strongly to an H_2O molecule whereas the eigen cation is created after binding one H_3O^+ ion strongly to three H_2O molecules as illustrated in the schematic diagram of **chart 1(b)** and **chart 1(c)** respectively, where the hydrogen bonds (hereafter, H−bonds) are represented by broken lines. Alike very significant role of the H_3O^+ ions in diffusing proton through the Grotthuss mechanism, the zundel and eigen cations are also found to be involved in proton transport and proton−hopping processes. Though the details of these mechanisms are still in contradiction, these two hydrated protons are believed to undergo inter−conversion between themselves: Eigen to Zundel to Eigen (E−Z−E), and Zundel to Zundel (Z−Z) [6], [7]. This phenomenon has been widely assumed to be a significant mechanism for explaining high conductivity of the protons in fuel cells and batteries, renewable energy materials, proton exchange membranes (hereafter, PEMs), anion exchange membranes etc. More importantly, it is extensively considered as a major proton migration mechanism in the Nafion series PEMs which are quite demanding proton conducting polymer films for operating fuel cells, redox flow battery systems, electrolysers etc. [8], [9].

Due to the involvement of mostly these three states of the hydrated protons in proton diffusion processes and their mutual inter−conversion mechanisms, intense research works have been carried out on their electronic structures and stabilities along with their critical role in proton diffusion mechanisms for nearly 220 years since de Grotthuss firstly proposed the fundamental assumptions of Grotthuss mechanism in 1806 [10]. Since then several structural data sets for clarifying electronic and structural stabilities of H_3O^+, $H_5O_2^+$, and $H_9O_4^+$ hydrated states, and interpreting a main Grotthuss's assumption: "the H−bond of these hydrated protons must be cleaved prior to drive protons forward" have been put forward [11], [12], [13], [14]. Even in this study as well, the same electronic stabilization of the protons by variable number of water molecules, and their mutual interactions in the aqueous solutions are investigated but with more distinctive, apparent, and comparative ways. The uniqueness of this insight lies in investigating electronic stabilities, ground state electronic structures, and three dimensional (hereafter, 3D) molecular geometries of the H_3O^+, $H_5O_2^+$, and $H_9O_4^+$ hydrated protons through more reliable three dimensionally distributed electron density surface mapping (mapped with the total density) techniques, and in seeking their chemical energetics plus binding energies for the sake of elucidating thermodynamic stability of them. Generally, in proton hydration mechanisms, it is very obvious that the water molecules around the H^+ ion move closer to latter under the influence of their mutual attractive force, and while interacting them to each other, a small change in total electronic energy of these microscopic particles occurs. But, such a small change in total electronic energy is very significant while accounting for the chemistry of these hydrated proton structures in the aqueous type solutions, and probing their structural, thermodynamic, and energetic stability in terms of ground state electronic energies. Therefore, it must be evaluated quite properly by some means so that one can reveal consistently better ground state molecular structure, 3D electron density surface map, and structural binding energy for each microhydrated proton. In theoretical research, an *ab initio* type quantum mechanical model has been accepted worldwide as the best alternative computational approach for incorporating such a small change in total electronic energy of the microhydrated cationic and anionic systems while optimizing their hydrated structures computationally [15], [16]. Accordingly, present study has employed a hybrid density functional B3LYP method with 6−31G (*d*, *p*) basis set, and applied explicitly to

H_3O^+, $H_5O_2^+$, and $H_9O_4^+$ hydrated states (as optimizing more bigger hydrated clusters by such *ab initio* type method is computationally expensive), and produced their respective global minimum electronic structures, and ground state energies theoretically, and determined the binding energy for each hydrated proton. Again, the same quantum mechanical model is used while computing their ground state vibrational frequencies at a particular nuclear Cartesian coordinate of their optimized structures (stationary point) and examined whether they truly represent global minimum of the potential energy surface or not. In fact, both of these computational techniques (geometry optimizations and frequency calculations) produce very trustworthy results that may ease us greatly while elucidating experimentally observed evidence quantitatively. With this, the present insight is organized as follows: The Computational methods are outlined in section 2, Results and Discussions are presented in section 3, and Conclusions are given in section 4.

II. Computational Details

In order to account for the electronic and structural stability of all the three hydrated states of the proton: H_3O^+, $H_5O_2^+$, and $H_9O_4^+$, the starting (trial) structures for geometry optimization of each of them were carefully built by using *GaussView*: the Gaussian graphical interface [17], and the respective Cartesian coordinates of the atoms were extracted. All these three trial structures were constructed by mimicking their IR and MD simulation generated molecular models displayed in **chart 1**. For each geometry optimization process, all the *Gaussian* keywords and methodologies were selected as instructed in *Gaussian 09* manual [20]. The hybrid functional based DFT method known as B3LYP was used with the basis set of this type: 6−31G (*d*, *p*) i.e. the methodology used was DFT: B3LYP/6−31G (*d*, *p*). The better and more reliable computational results were assured by using the greater basis set of the type 6−31G (*d*, *p*), where "6−31G" is the standard, split-valence double−zeta basis set: the functions that were used in *Gaussian* script computationally while describing the core and valence orbitals of the atoms; and the functions in parentheses "(*d*, *p*)" are polarization functions on heavy atoms and hydrogen. Besides computing ground state electronic energies for each hydrated proton structure, the electronic energies for the H^+ and H_2O systems were also determined by the same computational methodology and estimated the binding energy prior to predict thermodynamic stability of each hydrated proton theoretically. As the ionic specimens H^+, H_3O^+, $H_5O_2^+$, and $H_9O_4^+$ have charge unit = +1 each, and the molecular specimen H_2O has charge unit = 0, the respective set of integers (charge, spin multiplicity) used in their *Gaussian* input file was (1, 1), (1, 1), (1, 1), (1, 1), and (0, 1) respectively. Moreover, while solving the electronic Schrodinger equation iteratively, the self−consistent field (hereafter, SCF) with both default SCF procedure (SCF=Tight) and Berny algorithm for optimizations to a local minimum were selected in *Gaussian* 09 [18], [19]. To verify the theoretically converged geometry of each H_2O, H_3O^+, $H_5O_2^+$, and $H_9O_4^+$ as energetically minimum structure, the ground state frequencies (*Gaussian* keyword: *Freq*) for each optimized structure were calculated computationally by using the atomic Cartesian coordinates of the concerned geometry without changing computational methodology and basis set [18], [19], [20]. For this confirmation, the terminology "imaginary frequencies (negative signs)" was carefully searched in each *Gaussian* output file. But, in any case, if it was found, the new trial structure for the specific molecular specimen was built computationally and repeated the same *Gaussian* geometry optimization and frequency calculation procedures until no negative frequency was found. Moreover, while extracting three dimensionally displayed chemical data and visualizing each optimized geometry in the 3D space, the *Gaussian* output files (*.log*, *.fchk*, and *.chk*) of each molecular/ionic specimen were read by *GaussView*.

III. Results And Discussions

Generally, in chemistry, physics, and material science, more reliable ground state electronic energies and concerned 3D structures of the multi−electron and/or many−body giant atomic or molecular systems can be achieved through the quantum mechanical computations based on first principles DFT method [15], [16], [21], [22], [23], [24]. This is because unlike in *ab initio* method, there is a significant association of molecule's spatially dependent ground−state electron density (Hohenberg−Kohn theorem) in the DFT model where a functional is an electron density itself a function of space and time [20], [25], [26]. In terms of computational memory and occupied disk−space, this model is a cheap yet decent theoretical scheme involving repetitive complex−mathematical procedures which on the fly compute wave function and energy at a starting (trial) molecular geometry, test various possibilities to see which atomic arrangements and the electrons around them give the lowest energy value, determine the magnitudes of several physical observables quantitatively, and then proceed towards yielding a low energy ground state electronic structure and the concerned eigenvalues [20], [25]. In spite of its approximate formalism for solving Schrodinger's wave equation iteratively [27], the increasingly successful trend of it is mainly due to the inclusion of the Hohenberg−Kohn theorem that has a good ability for generating far better

results than the *ab initio* electronic structure methods at the similar computational cost. More specifically, the performance of this model is awesome while applying to microhydrated ions as reported earlier by the same author elsewhere [15], [16]. In these scientific reports, the author has highlighted the utmost potentiality of the DFT model, and underscored its skills to offer quite impressive explanation for elucidating experimentally observed molecular physicochemical properties of the microhydrated ionic kosmotropes such as $[SO_4^{2-}(H_2O)_n]$ n = 0−4, and 16, [15] and ionic chaotropes such as $[HSO_4^{-}(H_2O)_n]$ n = 0−3, and 5 [16]. As the present study is mainly concentered on computing low energy electronic structures and the concerned eigenvalues for the low charge density microhydrated protons such as Hydronium (H_3O^+): $[H^+(H_2O)]$, Zundel ($H_5O_2^+$): $[(H_3O)^+(H_2O)]$, and Eigen ($H_9O_4^+$): $[(H_3O)^+(H_2O)_3]$, and estimating their total structural binding energies, the same theoretical (i.e. DFT) model could be a very promising computational algorithm more especially for incorporating total change in electronic energies that occurs while interacting the micro−particles (H^+ and H_2O) to each other during hydration process of the protons in aqueous type media. All the concerned DFT derived results for these microhydrated ionic specimens are presented in the following subsections separately.

3.1 Electronic Stability of Hydronium ion (H_3O^+): $[H^+(H_2O)]$

The monohydrated H^+ ion i.e. $[H^+(H_2O)n]$, n = 1 (hydronium ion) has one molecule equivalent of water in the immediate vicinity of the H^+ ion. The DFT optimized geometry of it in gas phase is shown in **Figure 1a**, where red colored spheroid represents Oxygen (O) atom, and ash−grey spheroids represent Hydrogen (H) atoms respectively. Since in theoretical/ computational chemistry, the optimized geometry is mostly specified in reference to the following structural parameters: a) bond length: an intermediate distance between the two bonding atomic nuclei in any given molecule; and b) bond angle: an angle formed by three atomic nuclei across the two bonds, the explicitly measured dimension of each O−H (1O−2H, 1O−3H, and 1O−4H) bond length in DFT produced gas phased H_3O^+ structure is 0.982 Å, slightly shorter than the O−H bond length (= 1.0 Å) of H_2O in bulk water; and each equilibrium H−O−H bond angle (∠2H−1O−3H, ∠3H−1O−4H, ∠2H−1O−4H) is 113.5°, significantly greater than the H−O−H bond angle of H_2O (104.5°) in bulk water. Interestingly, these DFT derived values for the gas phased H_3O^+ ion are quite consistent to the simplest type first principle electronic structure calculation scheme; HF/6−31G (*d*, *p*) derived values: each O−H bond length and H−O−H bond angle is reported as 0.961 Å, and 114.7° respectively [28], and infra−red spectroscopy derived H−O−H bond angle 113° [29], laser absorption spectroscopy derived O−H bond length = 0.98 Å [30]. If we analyze these DFT derived structural data sets carefully, it can be predicted that the H_3O^+ ion has three equivalent and equioriented protons lying in the 3D space bound to the central O atom through quite strong bonding interactions, even stronger than that in the H_2O molecule. A comparatively high strength of the O−H bonding in H_3O^+ ion is quite reasonable as the bonding principle says: a shorter bond length means a stronger bond and vice versa i.e. atoms that are closer to each other mostly form strong covalent bonds, and those that are far apart to each other form weak bonds. As the central O atom of H_3O^+ ion has six valence electrons (Z = 8: $1s^2,2s^2 2p^4$) out of which two are equally shared with the two H atoms forming 2O−H covalent bonds, and a pair is donated to a proton forming a co−ordinate covalent bond (chart 1(a)), the remainder one electron pair remains as a lone pair. Thus, there are in total four pair electrons around the central O atom of the H_3O^+ ion. If we represent such electronic bonding patterns by the conventional AXE method where A, X, and E stand for the central O atom, number of O−H bonding pairs (=3), and number of lone pair (=1) respectively, the generic formula for the H_3O^+ ion must be AX_3E which is associated with the pyramidal type Lewis molecular structure. However, while referring this bonding model to valence shell electron pair repulsion (VSEPR) theory, the H_3O^+ ion must assume the shape of distorted pyramidal due to a stronger repulsive effect of the oxygen lone pair electron to the three O−H bonding pairs than the repulsion takes place in between themselves. Again, if we closely observe the DFT derived angular 3D orientation of each O−H bond of the H_3O^+ ion displayed in Figure 1 (a), it can be viewed as a flattened structure like a wind−blown umbrella whose handle points towards the localizing site of the oxygen lone pair. In terms of molecular symmetry, this O centered ion must belong to the symmetry group designated C_{3v} because of its three−fold axis (dimension of each equilibrium H−O−H angle is closed to 120°) with $3\sigma V$ planes along three O−H bonds.

In order to examine above mentioned bonding scenario, geometrical patterns, and a closed three dimensional molecular geometry more precisely, an electron density map (mapped with the total density) for the concerned optimized geometry must be used in theoretical chemistry. As a rule, this map is highly applicable to visualize the areas where electrons are present and where they are not, it in turn leads to image an exact molecular shape in the 3D space. This electron density map (transparent mode) for the H_3O^+ ion is

displayed in Figure 1(b), where charge distributions around the ion is clearly illustrated three dimensionally. It demonstrates well about the position of all the three centrally bound O−H bonds whose electron densities are found to be distributed symmetrically around the central O atom. The same can be speculated by the appearance of three clearly distinguishable protrusions (electron dense regions, indicated by three white colored arrows in Figure 1(b)) at the pyramidal base of the H_3O^+ structure. The next quite distinctive protrusion (shown by a red colored arrow) is appeared due to the presence of a lone pair electron on the central O atom as explained by the electronic theory of bonding earlier. As a whole, this total electron density surface has reconfirmed the flattened 3D structure (wind−blown umbrella) of the H_3O^+ ion in a more quantitative way.

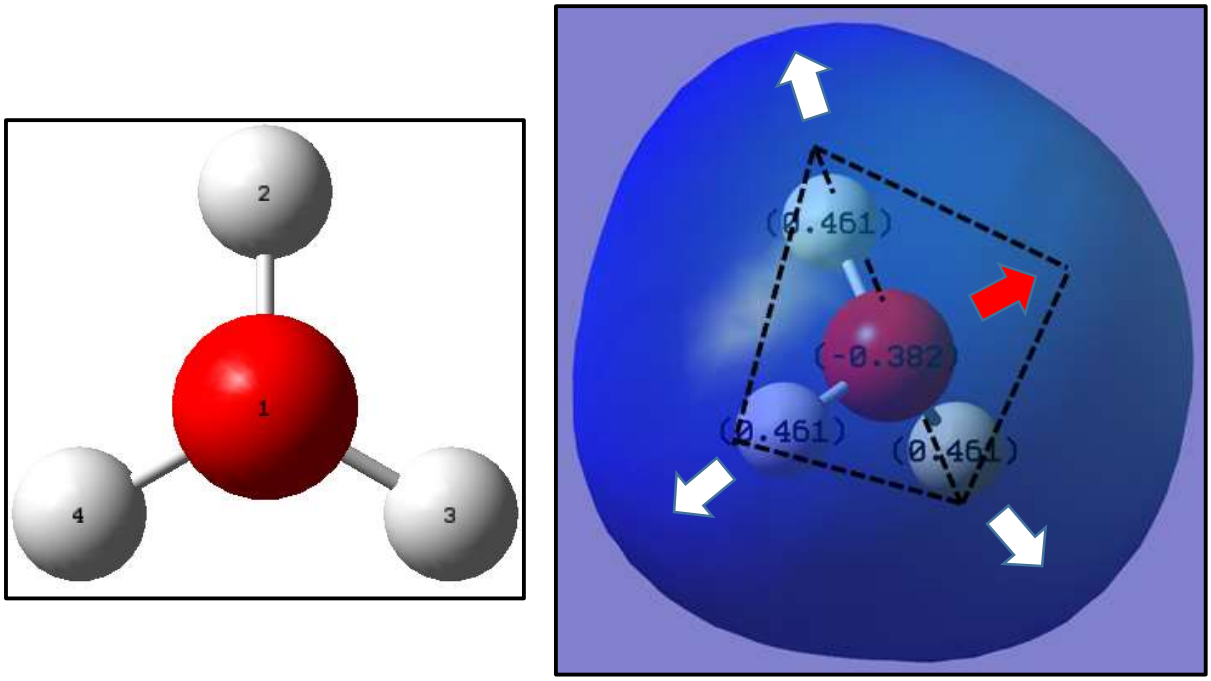

Figure 1. (a) A DFT optimized geometry of hydronium H_3O^+ ion. The ash−grey and red colored spheroids represent Hydrogen (H), and Oxygen (O) atoms respectively. For simplicity, a formal charge of the ion is omitted, and all the atoms are labeled numerically. (b) A DFT produced electron density map (mapped with total density; transparent mode) of H_3O^+ ion. The numeral values on the atoms represent partial atomic charges. The four arrow shapes indicate electron dense regions (protrusions) present around the central O

3.2 Electronic Stability of Zundel ion ($H_5O_2^+$): [$(H_3O)^+(H_2O)$]

Whenever a hydronium ion H_3O^+ is associated with one molecule equivalent of water in its immediate environ, the next possible hydrated proton [$H_3O^+(H_2O)n$], n = 1 called zundel ion is produced in the aqueous type solution at ambient temperature range. The DFT optimized geometry of it in gas phase is shown in Figure 2a, where red colored spheroids represent Oxygen (O) atoms, and ash−grey spheroids represent hydrogen (H) atoms respectively. As mentioned earlier in section 3.1, the real structures of the theoretically/computationally produced geometry of the molecular or ionic specimens can only be envisioned if we have got exact dimensions of the different types of bond lengths and bond angles. For the $H_5O_2^+$ ion, the explicitly measured values of different types of the bonds present are listed as: each O−H (1O−H3, 1O−H2, 4O−H6, 4O−H7) bond length is 0.971 Å, slightly shorter than the O−H bond length (= 1.0 Å) of H_2O in bulk water system and the O−H bond length (= 0.982 Å) of the gas phased H_3O^+ ion; each O---H (H−bond: 4O−H5, 1O−H5) type bond is 1.20 Å, significantly shorter than the H−bond length (= 1.80 Å) between two H_2O molecules (intermolecular hydrogen bond) in bulk water; and the distance between the O atoms (1O & 4O) of two H_2O molecules is 2.40 Å, notably shorter than the O−O distance (= 2.80 Å) between the two hydrogen bonded H_2O molecules in bulk water. As the central hydrogen atom 5H is shared with the two O atoms of two H_2O molecules by forming two identical H−bonds, the hydrated ion of this type can be called as symmetric H−bonded structure of the zundel ion

(asymmetric type zundel ion has not been considered here). More importantly, these DFT derived structural values for the gas phased $H_5O_2^+$ ion are found to be quite consistent with the experimentally and multi−configurational self−consistent field (MCSCF) derived values: each O−H and O---H (H−bond) bond length is reported as 0.95 Å [31] and 1.18 Å [32] respectively. Similarly, the concerned bond angles of the $H_5O_2^+$ ion are: each equilibrium H−O−H angle except the H atom involved in the H−bonding is 109.9°, significantly smaller than that in the H_3O^+ ion (H−O−H = 113.5°) and greater than in the H_2O (104.5°) of bulk water system; and the angle corresponding to that H−bonded atom 1O−5H−4O is measured as 174.2°, slightly smaller than the same type of intermolecular bond angle (O−H−O = 180°) present in bulk

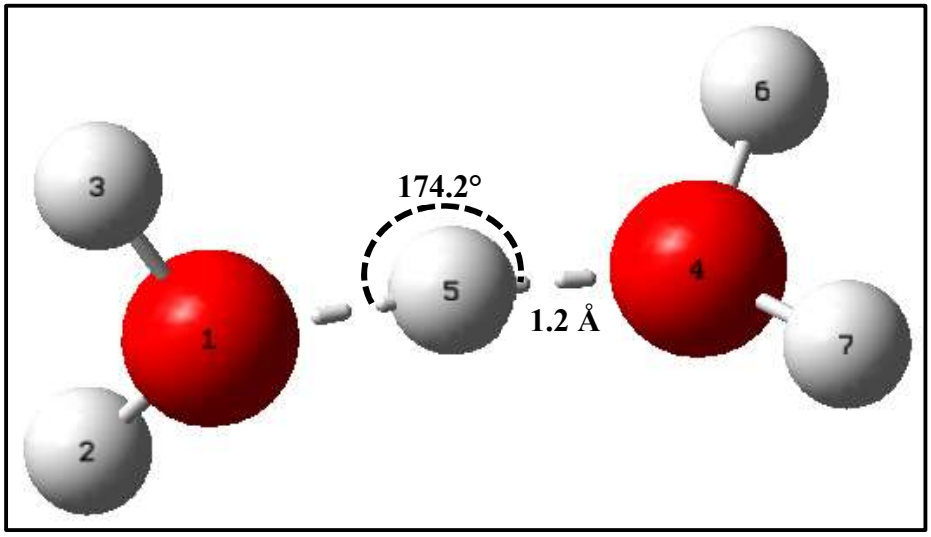

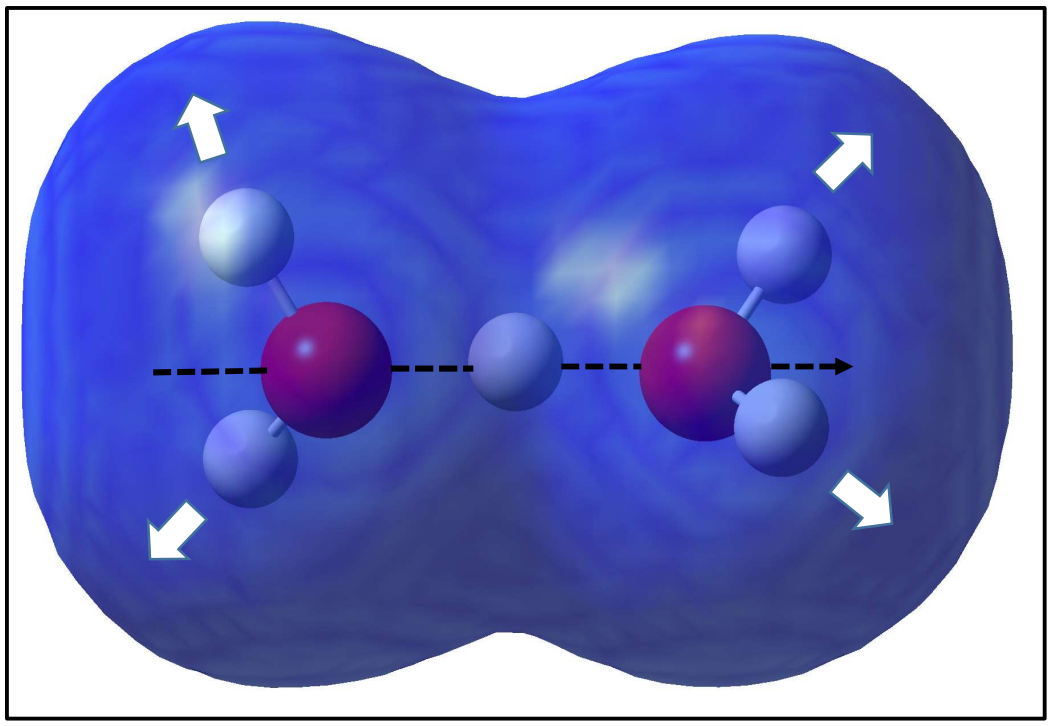

Figure 2. (a) A DFT optimized geometry of zundel $H_5O_2^+$ ion. The ash−grey and red colored spheroids represent Hydrogen (H), and Oxygen (O) atoms respectively. For simplicity, a formal charge of the ion is omitted, and all the atoms are labeled numerically. (b) A DFT produced electron density map (mapped with total density; transparent mode) of $H_5O_2^+$ ion. The four arrow shapes indicate electron dense regions (protrusions) present around the O atoms of two sideways H_2O molecules.

water. This slightly non−linear type bond angle in $H_5O_2^+$ ion is again due to the presence of H−bonded and symmetrically shared hydrogen atom in the central position of two H_2O molecules (Figure 1(a)) unlike in bulk water system where H−bond exists in between two nearby H_2O molecules. While analyzing these structural data sets carefully, one can predict that the $H_5O_2^+$ ion has four equivalent and equioriented protons (2H, 3H, 6H, and 7H) lying in the 3D space bound to the two central O atom (1O, and 4O) of two H_2O molecules with quite strong bonding interactions, and a proton (5H) is shared symmetrically in between two H_2O molecules with comparatively weaker hydrogen bonding interactions. Again, the DFT derived comparatively shorter bond length of each covalently bonded O−H bond of the $H_5O_2^+$ ion indicates higher O−H bond strength than that present in the H_3O^+ ion and H_2O molecule. Alike in H_3O^+ and H_2O, the central O atom of each sideways H_2O molecule of $H_5O_2^+$ has six valence electrons (Z = 8: $1s^2,2s^2 2p^4$) out of which two are equally shared with the two H atoms forming 2O−H covalent bonds, the remaining two pair electrons exist as lone pairs. Therefore, there are in total four pair electrons around the central O atom of each sideways H_2O molecule. If we represent such electronic bonding patterns by the conventional AXE method as we did for H_3O^+ ion in section 3.1, the generic formula for each sideways H_2O will be AX_2E_2 which is associated with the bent type Lewis molecular geometry. However, while referring this geometry prediction model to the VSEPR theory, each sideway H_2O must assume a V−shaped geometry due to a stronger repulsion between the two lone pair electrons present on each O atom that further repels the two O−H bonding pairs inwards resulting the distortion in the H−O−H bond angles. While incorporating equilibrium 1O−5H−4O bond angle, the zundel state must have a slightly distorted linear and flat structure with two V−shaped H_2O molecules at each side of the almost linear axis. This is an actual reason why such hydrated state of the proton always prefers to lie flat with C_{2v} symmetry while adsorbing on the metal surface [33].

Moreover, as for the H_3O^+ ion, the electron density map (mapped with the total density) for the DFT optimized geometry of the $H_5O_2^+$ ion has been used here to examine its above mentioned bonding scenario, geometrical patterns, and a closed three dimensional molecular geometry more precisely. As this map is highly practical to conceptualize the areas where electrons/charges are distributed mostly and where they are not, the exact molecular shape of the $H_5O_2^+$ ion in the 3D space can be envisioned more clearly. This type of electron density mapping (transparent mode) for the $H_5O_2^+$ ion is displayed in Figure 2(b), where charge distributions around the ion are clearly illustrated three dimensionally. It demonstrates well about the position of all the four centrally inbound O−H bonds of two sideways H_2O molecules whose electron densities are found to be distributed symmetrically around each central O atom. The same can be speculated due to the appearance of four clearly distinguishable protrusions (electron dense regions, indicated by four white colored arrows in Figure 2(b)) at the two sides of the almost linear horizontal axis. The next quite distinctive inward bound of the density surface appeared at the center discloses the fact about the centralization of bonding electron densities of the central H atom (5H) and two O atoms (1O and 4O) of the two sideways H_2O molecules. As a whole, this dumbbell shaped total electron density surface reconfigured the VSEPR derived distorted linear and flat structure of the symmetric type $H_5O_2^+$ ion in a more quantitative perspective.

3.3 Electronic Stability of Eigen ion ($H_9O_4^+$): [$(H_3O)^+(H_2O)_3$]

As explained in subsection 3.2, the positively charged hydronium ion H_3O^+ very often interacts strongly with the oxygen atoms of nearby H_2O molecules in the liquid phase. If the three molecule equivalent of water is internally linked with the central H_3O^+ ion to a greater extent, one more stable state of the proton $[H_3O^+(H_2O)n]$, $n = 3$ called eigen cation is produced in the aqueous type solution at ambient temperature range. The DFT optimized geometry of it in gas phase is shown in Figure 3a, where red colored spheroids represent Oxygen (O) atoms, and ash−grey spheroids represent hydrogen (H) atoms respectively. Just like in the case of hydronium and zundel cations, estimating the precise dimensions of the structural parameters such as bond lengths and bond angles is quite essential to conceptualize the proper geometry of the eigen cation in the 3D space. The explicitly measured values of the different types of bonds present in the eigen state $H_9O_4^+$ are listed as: each O−H (1O−3H, 1O−2H, 1O−4H) bond length of the central H_3O^+ ion is 1.02 Å, as equal as the O−H bond length (= 1.0 Å) of H_2O in bulk water system but slightly greater than the O−H bond length (= 0.982 Å) of the gas phased H_3O^+ ion and the O−H bond length (=0.971 Å) of the gas phased $H_5O_2^+$ ion; each O---H (H−bond: 11O−3H, 5O−4H, 8O−2H) type bond is 1.53 Å, significantly shorter than the H−bond length (= 1.80 Å) exist in between two H_2O molecules (intermolecular hydrogen bond) in bulk water but longer than the H−bond (= 1.20 Å) exists in $H_5O_2^+$ ion; the distance between the O atoms (1O & 11O, 1O & 5O, 1O & 8O) of central H_3O^+ ion and three H−bonded H_2O molecules is 2.55 Å, notably shorter than the O−O distance (= 2.80 Å) between the two H−bonded H_2O molecules in bulk water but longer than that for the $H_5O_2^+$

ion (1O & 4O distance = 2.40 Å); and each O−H bond length present in the three H−bonded H_2O molecules is 0.965 Å, slightly smaller than the O−H bond length (= 1.0 Å) of hydrogen bonded H_2O in bulk water system. As each hydrogen atom (partially positive charged) of the central H_3O^+ ion is undergone electrostatic attraction with the electronegative O atom of the three nearby H_2O molecules, and all these three H_2O molecules are equally spaced and symmetrically distributed around the centrally located H_3O^+ ion, the whole hydrated form can be envisioned as a symmetric type H−bonded structure of the eigen proton. While comparing these DFT derived structural parameters' values of the gas phased $H_9O_4^+$ ion with the available experimental values reported elsewhere [34]: each O−H & O---H (H−bond) bond length, and O−O distance is reported as 0.98 Å, 1.61 Å, and 2.59 Å respectively, they are found to be quite consistent to each other. Similarly, the accessible bond angles of the $H_9O_4^+$ ion are: each equilibrium H−O−H bond angle of the central H_3O^+ ion is 112.8°, smaller than that in the H_3O^+ ion (H−O−H = 113.5°) but greater than in the H_2O (104.5°) of bulk water system; each 11O−1O−5O, 11O−1O−8O, and 5O−1O−8O (triangular) type angles are measured as 113.5° implying that the orientations of three H_2O groups adopt the positions of a slightly distorted triangle−113.5° apart in a plane; and each bond angle corresponding to H−bonded atoms 1O−3H−11O, 1O−4H−5O, and 1O−2H−8O is measured as 175.5°, slightly smaller than the same type of intermolecular bond angle (O−H−O = 180°) in bulk water. Such little bit non−linear type bond angles in $H_9O_4^+$ ion are again due to the presence of H−bonded and symmetrically shared three hydrogen atoms in the central position of three surrounding H_2O molecules (Figure 3(a)) unlike in bulk water system where the H−bond does exist in between two nearby H_2O molecules, and in $H_5O_2^+$ ion where two H−bond exists in between central H atom and two nearby sideways H_2O molecules (Figure 2(a)). While analyzing all of these structural data sets thoughtfully, we can predict that the $H_9O_4^+$ cation has six equivalent and equioriented protons (6H, 7H, 9H, 10H, 12H, and 13H) lying in the 3D space bound to the three central O atom (11O, 8O, and 5O) of three triangularly distributed H_2O molecules through the quite strong covalent type bonding interactions, and three similar type protons (2H, 3H and 4H) but bound to the O atom of the central H_3O^+ ion that remains connected symmetrically with the three neighboring H_2O molecules via comparatively weaker hydrogen bonding interactions. Moreover, comparatively shorter H−bond length of the $H_9O_4^+$ ion than that exists in between two H_2O molecules in bulk water system implies that an intermolecular binding force in former ion is stronger than in the latter. The detailed chemical energetics and the thermodynamic stability of this eigen state has been elucidated in subsection 3.4. Furthermore, alike in the zundel state, the central O atom of each H−bonded H_2O molecule of the eigen state has six valence electrons (Z = 8: $1s^2,2s^2 2p^4$) out of which two are equally shared with the two H atoms forming 2O−H covalent bonds, the remaining two pair electrons subsist as lone pairs. Therefore, there are in total four pair electrons around the central O atom of each triangularly arranged H_2O molecule. While representing such electronic bonding patterns by the conventional AXE method, the generic formula for each triangularly arranged H_2O is AX_2E_2 which is associated with the bent type Lewis molecular shape. However, while referring this geometry prediction model to the VSEPR theory, each triangularly arranged H_2O must assume a V−shaped geometry as explained earlier in section 3.1. If we include all the three equilibrium 11O−3H−1O, 5O−4H−1O, and 8O−2H−1O type bond angles, it can be depicted that the eigen state must have a central H_3O^+ ion connected almost linearly to the triangularly placed three V−shaped H_2O molecules via three H−bonds giving a whole structural unit as a distorted trigonal planar shape. This is an actual reason why such hydrated state of the proton always lies triangularly or occupies triangular space while adsorbing on the metal surface such as Pt(111) [35].

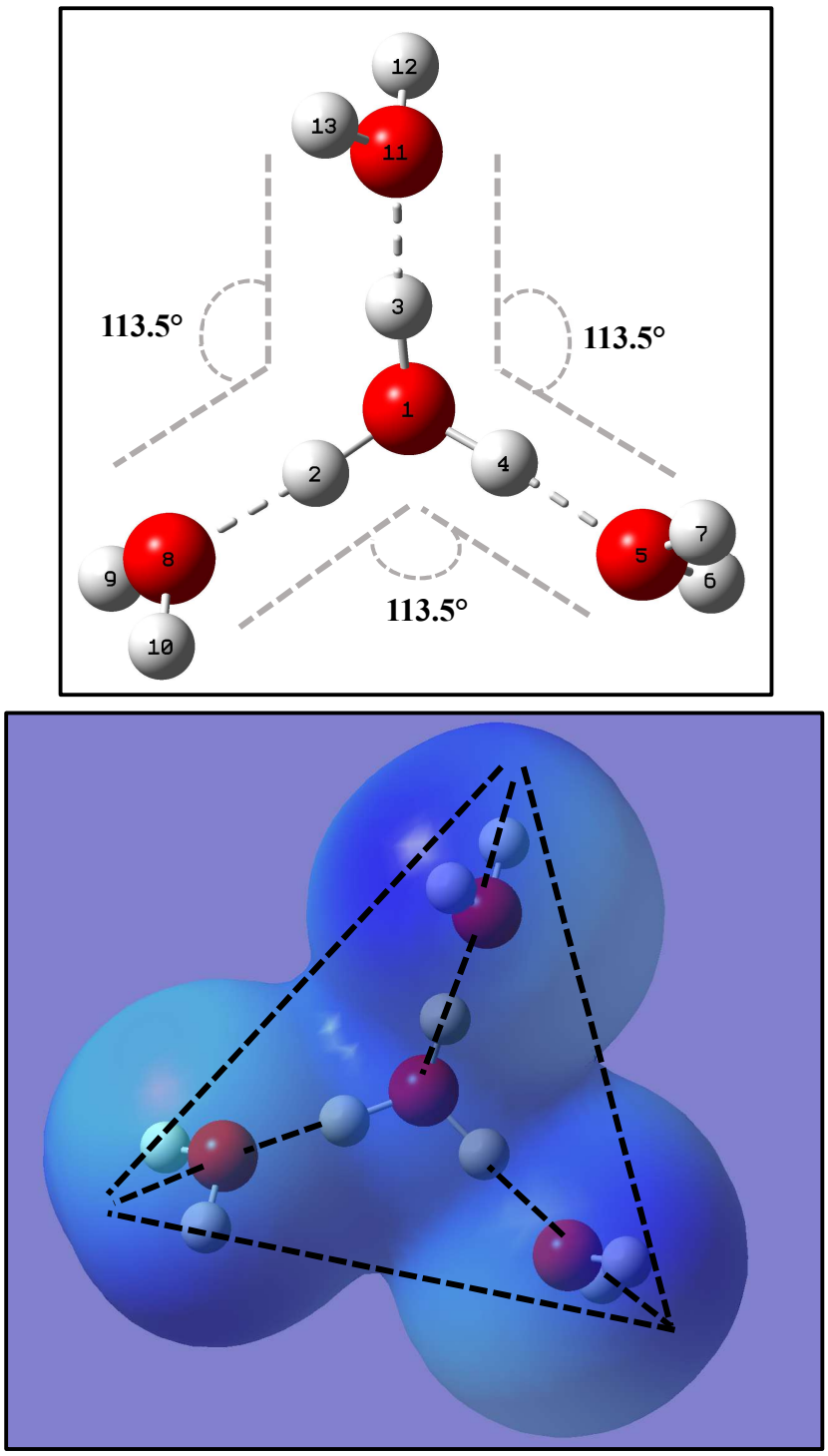

Figure 3. (a) A DFT optimized geometry of eigen $H_9O_4^+$ ion. The ash−grey and red colored spheroids represent Hydrogen (H), and Oxygen (O) atoms respectively. For simplicity, a formal charge of the ion is omitted, and all the atoms are labeled numerically. (b) A DFT produced electron density map (mapped with total density; transparent mode) of $H_9O_4^+$ ion. The three triangularly distributed electron dense regions (protrusions) present around the central H_3O^+ ion approximate the location of three H_2O molecules.

Again, as for the zundel and hydronium ions, the electron density map (mapped with the total density) for the DFT optimized geometry of the eigen ion is used here to examine its above mentioned geometrical patterns, and a closed three

dimensional molecular geometry more accurately. Since, this map is highly practical while visualizing the areas where electrons or charges are distributed mostly and where they are not, the exact molecular shape of the $H_9O_4^+$ ion in the 3D space can be envisioned more clearly. This type of electron density mapping (transparent mode) for the $H_9O_4^+$ ion is displayed in Figure 3(b), where charge distributions around the ion are clearly seen three dimensionally. It demonstrates well about the triangular position of all the three centrally inbound H_2O molecules whose electron densities are found to be distributed symmetrically around the central H_3O^+ ion at each corner of the slightly distorted tringle. The next quite distinctive inward bound of the density surface appeared at the center of each side of the triangular shape reveals that the bonding electron densities of each H (2H, 3H, and 4H) atom of the H_3O^+ and O atom (5O, 8O, and 11O) of the three triangularly arranged H_2O molecules are centralized. As a whole, this total electron density surface reassured the VSEPR derived distorted triangular planar geometry of the symmetric eigen proton in a more quantitative perspective.

3.4 Energetic Stability and Binding Energy

To reconfirm the above mentioned 3D geometry of all these three states of the proton: H_3O^+, $H_5O_2^+$, and $H_9O_4^+$ produced from the normal convergence procedure and computational termination by obeying all the DFT endorsed quantum mechanical criteria, the ground state frequencies were calculated by explicitly using the concerned atomic Cartesian coordinates of each DFT optimized geometry without changing computational methodology (B3LYP/6−31G (d, p)). Interestingly, no any imaginary frequencies (zero negative frequencies) were found successfully for all the DFT derived geometry of these three states of the hydrated protons. It assures that the DFT produced geometries of them displayed respectively in Figure 1, Figure 2, and Figure 3 represent a true minimum of their own potential energy surface (hereafter, PES) or these structures represent their most stable ground state electronic structures. As a rule, no appearance of the negative frequencies means the atomic Cartesian coordinates of the converged/optimized geometry of each of them do not move at all from their initial positions (concerned local minimum structure) while the frequencies (keyword: *Freq*) are being calculated computationally, further guarantying that these theoretically predicted lowest energy electronic structures of the hydrated protons truly represent a minimum of their PES. In terms of the technical sense in physical chemistry (thermodynamics and chemical energetics), the molecular or ionic systems are said to be in thermodynamically stable states whenever they are in their lowest energy states, and in terms of quantum mechanical perspective, the thermodynamically stable states means their ground states. Therefore, thermodynamic stability of any chemical systems or molecular/ionic specimens is directly related to their chemical and structural stability which in turn associates with their energetic stability and ground state energy terms. Again, the energetic stability of any substances increases with decreasing their potential energy, and the potential energy itself is a function of these relevant molecular features: bond strength, charge/electronic distributions, chemical compositions, intermolecular forces, states of matter etc. In theoretical chemistry, the DFT model is the best alternative quantum mechanical approach to the traditional Hartree−Fock (HF) or many−body perturbation theory (MP2), for incorporating the major effects of these significant parameters while computing ground state electronic energies of the molecular or ionic specimens [36]. In the present study, the DFT model was employed to derive ground state electronic energies of all the three hydrated states of the protons as summarized in Table 1 where binding energy (ΔE) for each of them has been calculated separately. In terms of their ground state electronic energies listed in the third column of Table 1, it can be said that the eigen state of the proton is energetically the most stable, the zundel state is second most stable, and the hydronium ion is the least stable state of the hydrated proton. So, thermodynamically as well, the eigen state of the proton is the most stable state and hence, is the *most predominant* hydrated *proton* species exist in liquid water systems. If we plot the positions of all these three states of the proton on an energy diagram, what it looks like is shown in Figure 4.

Moreover, one of the most commonly used strategies to achieve a more detailed understanding of the hydrated protons chemistry in bulk water is to investigate their binding energies in the gas phase. In ionic hydration chemistry, the binding energy (ΔE) is defined as an energy required to disassemble the hydrated molecular structures into their constituent molecules and ions [1]. It simply measures bond energy and bond−dissociation energy of the protons bound with the specific number of water molecules. Here, the DFT predicted electronic energies of the three stable hydrated protons are used to calculate their binding energies consecutively. The ΔE is mathematically formulated with the total electronic energy of the whole hydrated structure (E_T), electronic energy of the naked proton (E_{H^+}), and that of the water molecule (E_{H2O}) as: $\Delta E = [\, E_T - \{E_{H^+} + (E_{H2O} \times n)\}\,]$, where n stands for the hydration number of each state of the proton. The detailed calculations of ΔE value for each hydrated state of the protons is summarized in Table 1, where

all the DFT derived electronic energies and the mathematically calculated ΔE values are expressed in atomic units (*a. u.*). As a rule, larger the binding energy, higher is the structural stability, and more negative the ΔE values, more stable is the hydrated structure. It implies that an order of increasing relative stability of these three hydrated states of the proton is $H_9O_4^+ > H_5O_2^+ > H_3O^+$ as illustrated in the energy diagram shown in Figure 4.

Table 1. The DFT derived electronic energies and calculated binding energies (ΔE) for the hydronium, zundel, and eigen states of the proton.

Hydrated protons	Hydration number(n)	DFT derived electronic energies			*calc.* Binding Energies (ΔE)
		a. u.			
		Total (E_T)	E_{H+}	E_{H2O}	$\Delta E = [\, E_T - \{E_{H+} + (E_{H2O} \times n)\}]$
H_3O^+	1	−75.7056	0.00	−76.4197	+ 0.7141
$H_5O_2^+$	2	−153.1918	0.00	−76.4197	− 0.3524
$H_9O_4^+$	4	−306.1123	0.00	−76.4197	− 0.4335

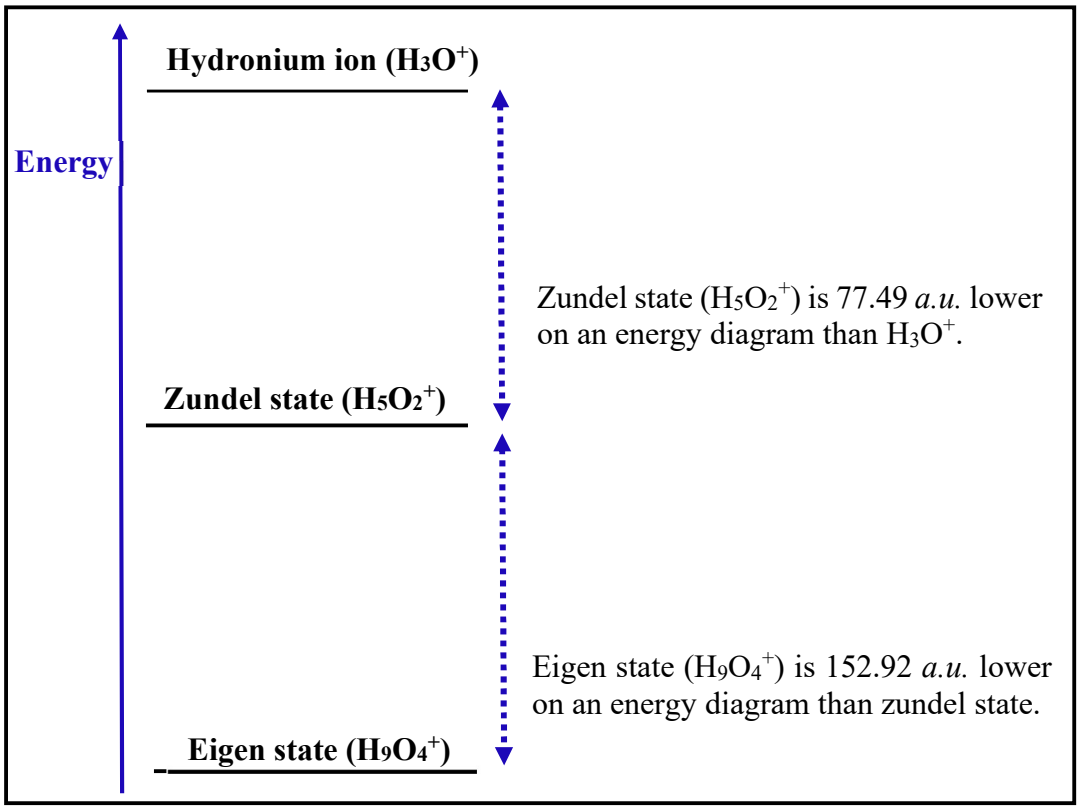

Figure 4. An energy diagram for three different hydrated states of the proton: H_3O^+, $H_5O_2^+$, and $H_9O_4^+$.

IV. Conclusion

This research work gave insight into the quantum−mechanical investigation of the electronic stabilities and the chemical energetics of the three most possible stable micro−hydrated states of the proton: hydronium ion H_3O^+, zundel ion $H_5O_2^+$, and eigen ion $H_9O_4^+$. Since the micro− hydration phenomenon of the protons simply deals with the inclusion of the discrete water molecules in the immediate environs of the protons and their mutual bonding interactions, the decisive role played by it

while computing electronic stabilities and ground state electronic energies at the atomic levels was addressed quantitatively by employing computationally cheap yet decent density functional theory (DFT) model. Firstly, the ground state electronic structures and the concerned electronic energies of each of these three hydrated protons were determined, and then inquired of their thermodynamic stabilities. It is found that almost all the theoretically estimated structural (bond lengths and angles) dimensions of the DFT produced three-dimensional electronic structure of each hydrated proton are closed and consistent with the available experimental data sets. By realizing this accuracy level, many experimentally undetermined yet but theoretically predicted (in this work) structural data sets are claimed here as the most precise and accurate data values. Structurally, the H_3O^+ ion is theoretically predicted as a flattened 3D structure (wind−blown umbrella) with C_{3v} symmetry, the symmetric type $H_5O_2^+$ ion as a linear and flat structure with C_{2v} symmetry, and the symmetric $H_9O_4^+$ ion as a triangular planar structure. All these geometrical shapes, and the closed three dimensional molecular geometries were examined more closely through electron density mapping (mapped with the total density) techniques, and reconfirmed each and every 3D molecular geometry quantitatively. Again, the ground state frequencies for the DFT derived geometry of each hydrated proton were computed theoretically (B3LYP/6−31G (*d*, *p*)), and reassured their lowest energy electronic structures that can truly represent a minimum of their potential energy surface. Besides this, the thermodynamic stability of these hydrated protons was analyzed on the basis of their DFT derived ground state electronic energies, and revealed that the eigen state of the proton is the most stable state after which is the zundel state and then is the hydronium ion. In terms of theoretically calculated values of their binding energies, the same descending order in their relative thermodynamic stability ($H_9O_4^+ > H_5O_2^+ > H_3O^+$) was observed.

REFERENCES

[1] R. D. Madan, Modern Inorganic Chemistry (S. Chand & Company: India, 1997).

[2] D. M. Camaioni, C. A. Schwerdtfeger, *J. Phys. Chem. A* 109, 10795(2005).

[3] D. W. Lim, M. Sadakiyo, H. Kitagawa, *Chem. Sci.* 10, 16(2019).

[4] K. Mizuse, A. Fujii, N. Mikami, *J. Chem. Phy.* 126, 231101(2007).

[5] O. Markovitch, N. Agmon, *J. Phys. Chem. A* 111, 2253(2007).

[6] N. Agmon, *Chem. Phy. Lett*. 244(5), 456(1995).

[7] J. Han, H. Liu, *International Mechanical Engineering Congress and Exposition Proceedings*, 1(2005).

[8] Y.S. Park, T. Hatae, H. Itoh, M. Y. Jang, Y. Yamazaki, *Electrochimica Acta* 50(2−3), 592(2004).

[9] S. Banerjee, D. E. Curtin, *J. Fluorine Chem*. 125(8), 1211(2004).

[10] C. J. D. von Grotthuss, *Ann. Chim*. LVIII, 54(1806).

[11] J. M. Headrick, E. G. Diken, R. S. Walters, N. I. Hammer, R. A. Christie, J. Cui, E. M. Myshakin, M. A. Duncan, M. A. Johnson, K. D. Jordan, *Science* 308, 1765(2005).

[12] K. R. Asmis, N. L. Pivonka, G. Santambrogio, M. Brummer, C. Kaposta, D. M. Neumark, L. Wo¨ste, *Science* 299, 1375(2003). (b) M. Miyazaki, A. Fujii, T. Ebata, N. Mikami *Science* 304, 1134(2004). (c) J. W. Shin, N. I. Hammer, E. G. Diken, M. A. Johnson, R. S. Walters, T. D. Jaeger, M. A. Duncan, R. A. Christle, K. D. Jordan, *Science* 304, 1137(2004). (d) C. C. Wu, C. K. Lin, H. C. Chang, J. C. Jiang, J. L. Kuo, M. L. Klein, *J. Chem. Phys.*122, 074315(2005).

[13] J. C. Jiang, Y. S. Wang, H. C. Chang, S. H. Lin, Y. T. Lee, G. N. Schatteburg, H. C. Chang, *J. Am. Chem. Soc.*122, 1398(2000).

[14] M. Eigen, L. D. Maeyer, *Proc. R. Soc. London, Ser. A* 247, 505(1958).

[15] A.B. Marahatta, *Int. J. Prog. Sc. Tech.* 17(1), 55(2019).

[16] B. Marahatta, *Int. J. Prog. Sc. Tech.* 18(2), 43(2020).

[17] Æ. Frisch, H. P. Hratchian, R. D. Dennington II, T. A. Keith, J. Millam, Gauss view 05 Reference (Gaussian, Inc. 2009).

[18] Gaussian 09 manual. *http://gaussian.com/geom/?tabid=1#GeomkeywordReadOptimi HYPERLINK "http://gaussian.com/geom/?tabid=1"zeoption*

[19] Æ Frisch, Gaussian 09W Reference (Gaussian, Inc., 2009).

[20] J. B. Foresman, Æ Frisch, Exploring Chemistry with Electronic Structure Methods (Gaussian, Inc., 2015).

[21] A.B. Marahatta, *Int. J. Prog. Sc. Tech.* 20(2), 348(2020).

[22] B. Marahatta, *Int. J. Prog. Sc. Tech.* 19(2), 48(2020).

[23] B. Marahatta, *Int. J. Prog. Sc. Tech.* 19(1), 100(2020).

[24] W. Kohn, L. Sham, *Phys. Rev. J.* 140(4A), A1133(1965).

[25] P. Hohenberg, W. Kohn, *Phys. Rev. B* 136(3B), 864(1964).

[26] W. Kohn, L. Sham, *Phys. Rev. J.* 140(4A), A1133(1965).

[27] A.J. Cohen, P. M. Sánchez, W. Yang, *Science* 321(5890), 792(2008).

[28] J. M. Hermida-Ramón, G. Karlström, *J. Mol. Struct.* (*Theochem*) 712, 167(2004).
[29] J. Tang, T. Oka, *J. Mol. Spec.*196(1), 120(1999).
[30] T. J. Sears, R. Bunker, B. Davies. A. Johnson, *J. Chem. Phys.* 83(6), 2676(1985).
[31] P. L. Silvestrelli, *J. Chem. Phy.*146, 244315(2017).
[32] F. F. Muguet, *J. Mol. Str*. (Theochem) 368,173(1996).
[33] P. Quaino, N.B. Luque, G. Soldano, R. Nazmutdinov, E. Santos, T. Roman, A. Lundin, A. Grob, W. Schmickler, *Electrochimica Acta* 105, 248(2013).
[34] A. Zavitsas, *J. Phys. Chem. B* 105, 7805(2001).
[35] Y. Kim, S. Shin, H. Kang, *Angewandte Chemie* 54(26), 7626(2015).
[36] G. Seifert, K. Krüger, Density Functional Theory, Calculations of Potential Energy Surfaces and Reaction Paths. In: Heidrich D. (eds) The Reaction Path in Chemistry: Current Approaches and Perspectives. Understanding Chemical Reactivity, vol. 16. (Springer, 1995).